ICJK

Journal of Advanced Materials Research
http://dx.doi.org/10.62762/JAMR.2026.813028

RESEARCH ARTICLE

Contact Inactivation of Human Adenovirus Type 5 by Silicon Nitride Ceramics

Ioannis Katsaros[1], Anette Carlsson[2], Cecilia Persson[3], Göran Akusjärvi[2], Xiaoli Liu[4], Wei Xia[1,*] and Håkan Engqvist[1]

[1] Division of Applied Materials Science, Department of Materials Science and Engineering, Uppsala University, Uppsala 751 05, Sweden
[2] Department of Medical Biochemistry and Microbiology, Uppsala University, Uppsala 751 05, Sweden
[3] Division of Biomedical Engineering, Department of Materials Science and Engineering, Uppsala University, Uppsala 751 05, Sweden
[4] School of Future Technology, Xi'an Jiaotong University, Xi'an 710049, China

Abstract

Preventing pathogen transmission and treating pathogen-associated diseases remain major public-health challenges. Recent epidemics and pandemics, key amongst them being the pandemic caused by the coronavirus disease (COVID-19), have highlighted the devastating effects that viral infections can have on society. Uncovering and utilising materials for the protection from and treatment of virus-induced diseases can considerably alleviate the load imposed on healthcare systems worldwide. Silicon nitride is a biocompatible ceramic material used in orthopedic implants that is effective in the inactivation of single-stranded RNA viruses. However, the effect of the material on the more resilient DNA viruses remains unknown. This study aimed to investigate the antiviral behaviour of the material, in powder and bulk form, against DNA viruses, and more specifically the human adenovirus. The results of the study indicated that silicon nitride dramatically reduces adenoviral infectivity in powder (>98% reduction in infective virus compared to the untreated control) and bulk form (>73% reduction in infective virus compared to the untreated control). In both cases, inactivation was achieved rapidly, in one minute for powders and 10 minutes for bulk surfaces. The findings of this study strengthen the potential of silicon nitride to be used as an antiviral agent, aiding the fight against the spread of both DNA and RNA virus diseases.

Keywords: silicon nitride, viral inactivation, surfaces, adenovirus.

1 Introduction

Pandemics and epidemics are recurring phenomena in human history [1–3]. The COVID-19 pandemic, which started in 2019 [4], is a reminder that humanity should be prepared for future pandemics caused by viruses.

Submitted: 05 July 2026
Revised: 31 August 2026
Accepted: 03 September 2026
Published: 12 September 2026

Vol. 2, **No.** 4, 2026.
10.62762/JAMR.2026.813028

***Corresponding author:**
✉ Wei Xia
wei.xia@angstrom.uu.se

Citation
Katsaros, I., Carlsson, A., Persson, C., Akusjärvi, G., Liu, X., Xia, W., & Engqvist, H. (2026). Contact Inactivation of Human Adenovirus Type 5 by Silicon Nitride Ceramics. *Journal of Advanced Materials Research*, 2(4), 274–284.

© 2026 by the Authors. Published by Institute of Central Computation and Knowledge. This is an open access article under the CC BY license (https://creativecommons.org/licenses/by/4.0/).

COVID-19, caused by the severe acute respiratory syndrome coronavirus 2 (SARS-CoV-2), has affected several million people [5] with a fatality rate that rises exponentially with patient age [2]. While personal responsibility, protective equipment and disinfectants are relatively effective in containing the spread of this novel coronavirus [6, 7], more measures should be taken to inhibit the rapid spread of such pathogens.

Antipathogenic materials can be important tools limiting the spread of viral diseases. Such materials can be used as disinfecting agents in protective equipment or to provide long-term inactivation of viruses on surfaces [3, 8] which carry a pathogenic load and contribute to the spread of disease [9, 10]. Copper is such a material, and studies prove that its use on high-touch surfaces considerably reduces the pathogenic load [11–13].

Silicon nitride could be another option. It is a ceramic material that has been utilised in applications where components are to be placed in thermally and mechanically challenging environments [14]. Its biocompatible nature [15, 16] and mechanical properties [17, 18] have led to its evaluation as a potential biomaterial. Today, silicon nitride has been approved for human use as a spinal implant with positive clinical results [19, 20] and shows promise in dental and other orthopedic applications [21, 22]. Unlike conventional bioinert ceramics such as alumina and zirconia, Si_3N_4 possesses biologically active surface chemistry, including potential antibacterial and osteogenic effects [23, 24].

Indeed, one of the main advantages of silicon nitride in orthopedic implants is its antibacterial behaviour, caused by the elution of ammonia ions and the formation of reactive nitrogen species (RNS) from its surface when in contact with water. These ions lead to bacterial inactivation, with literature confirming the antibacterial properties of the material *in vitro* and *in vivo* [23, 24]. This prompted investigations into this material for its antiviral properties, which proved that, in powder form, it is a potent inactivator of single-stranded RNA (ssRNA) viruses, including SARS-CoV-2 [25, 26]. While RNA viruses exhibit significantly higher mutation rates than DNA viruses due to the error-prone nature of RNA-dependent RNA polymerases [27], making them more difficult to vaccinate against, DNA viruses are generally more stable. To date, no investigation of the effects of silicon nitride on DNA viruses exists.

In contrast to the majority of RNA viruses, the human adenovirus (HAdV) is a naked virus lacking a membranous coat surrounding its core. This makes HAdV extremely stable compared to RNA viruses in a variety of environments [28]. HAdV can be transmitted through aerosols, faecal–oral transmission, or through contaminated surfaces, where it has been shown to remain viable for extended periods [29, 30]. Although most HAdV infections are self-limiting, fatal infections can occur in immunocompromised patients [31]. Furthermore, severe outbreak events have been documented, such as those caused by novel adenovirus serotypes leading to life-threatening pneumonia [32], and a high adenoviral load is correlated with more severe respiratory symptoms in intensive care units where adenoviral cross-infection has been noted [33].

To the best of our knowledge, the antiviral properties of silicon nitride have only been examined against RNA viruses. The aim of this study was to evaluate the antiviral potential of silicon nitride in both powder and bulk form against DNA viruses. The HAdV type-5 virus was chosen for its high resistance to physical or chemical agents and adverse conditions [34, 35]. It was speculated that any effect on the highly resilient adenovirus could be extended to other DNA viruses.

2 Materials and methods

2.1 Test materials and controls

To investigate the antiviral properties of silicon nitride against the human adenovirus, test samples and controls in both powder and bulk form were used.

For the testing of powders, silicon nitride (with a D_{50} of 856 nm and a surface area of 8.1 m^2/g) was purchased from Luoyang Tongrun Technology Co., Ltd (Henan, China). Copper was chosen as a positive control due to its widely accepted nature as an antipathogenic material [36, 37]. Copper powders were purchased from Sigma-Aldrich (St. Louis, MO, USA).

Similarly, to evaluate whether silicon nitride surfaces would lead to viral inactivation, samples were produced through spark plasma sintering according to Fu et al. [38]. Briefly, silicon nitride powders (Sigma-Aldrich, St. Louis, MO, USA) were milled for 3 hours at 350 rpm in a planetary ball mill together with 4 wt.% MgO, 4 wt.% SrO and 2 wt.% SiO_2 as sintering additives and ethanol as a wet-milling agent. The sintering additives were chosen as more bioactive and biocompatible alternatives to the commonly used yttria and alumina [38]. Approximately 2.5 g of the powders were then dried and placed in a graphite mould

(20 mm in diameter), where they were manually pressed into a disc. Finally, the powders were spark plasma sintered (SPS-825, Fuji Electronic Industrial, Japan) at 1720 °C under a constant pressure of 30 MPa with a dwell time of 5 minutes. Copper cubes (10 mm × 10 mm × 10 mm) (Aston Carlsson AB, Skogås, Sweden) were used as positive controls in this case. All powders and surfaces that were to be brought into contact with the virus were sterilised and handled using sterile procedures.

2.2 Material characterization

The morphology of the tested powders was examined using scanning electron microscopy (SEM) (Zeiss LEO 1550, Carl Zeiss, Jena, Germany) at an accelerating voltage of 5 kV and a working distance of approximately 5 mm. Silicon nitride powders and surfaces were sputter-coated with a conductive Au/Pd layer approximately 10 nm thick to facilitate imaging. The phase composition of all powders and surfaces was examined using X-ray diffraction (XRD) (D500, Bruker, Billerica, MA, USA). The samples were scanned from 10° to 80° (2θ) at a scanning rate of 0.02°/s. Furthermore, the surface roughness of all tested surfaces was measured by optical profilometry (Zygo, Middlefield, CT, USA). A square area of 167 µm × 167 µm was scanned using a 10× objective for silicon nitride and a 50× objective for copper. Three measurement areas were acquired per sample across five replicate samples per material type, yielding 15 measurements in total per material, after which the results were averaged. Finally, the release of copper ions from the copper powders was examined through inductively coupled plasma optical emission spectrometry (ICP-OES) (Avio 200, PerkinElmer, Waltham, MA, USA) in an effort to explain the observed time-dependent antiviral behaviour of copper. Suspensions containing 500 mg of the copper powder in 5 mL of deionised water (final concentration = 10% w/v) were prepared. These suspensions were placed in a rotary mixer for one minute, 10 minutes and one hour; they were then filtered and the copper ion concentration in the supernatants was measured through ICP-OES.

2.3 Cell culture and virus

Human lung adenocarcinoma cells (A549) (ATCC) were cultured in 10 cm Petri dishes in Dulbecco's Modified Eagle's Medium (DMEM) (Thermo Fisher Scientific, Waltham, MA, USA) supplemented with 10% fetal calf serum (FCS) (Thermo Fisher Scientific, Waltham, MA, USA) and 1% PenStrep (Thermo Fisher Scientific, Waltham, MA, USA) at 37 °C, 5% CO_2. The human adenovirus type-5 (HAdV-5) expressing the reporter firefly luciferase gene integrated into the non-essential E3 region [39] was used for the infection tests.

2.4 Pre-infection treatment

For the powder testing, 10% w/v suspensions of the test powders in 1 mL of serum-free DMEM were prepared in 1.5 mL microcentrifuge tubes. A volume of 8 µL of the viral solution (focus-forming units (FFU) $mL^{-1} = 2.7 \times 10^7$) was brought into contact with the Si_3N_4 or copper suspensions for one minute, 10 minutes and one hour, respectively, during incubation at 37 °C, 5% CO_2. As a negative control, 8 µL of the same viral solution was diluted in 1 mL of serum-free DMEM containing no powder. All vials were gently shaken every five minutes, where applicable, to ensure sufficient material–virus contact. After incubation, the vials were centrifuged at 8000 rpm for 5 minutes to separate the powders from the supernatant. The supernatant was then used to infect the A549 cells.

Regarding the surfaces, a similar protocol was followed. Test samples and positive controls were placed in individual wells of a six-well plate. Starting from the same viral solution, droplets of 8 µL were placed on the materials and incubated for 10 minutes and one hour, respectively, at 37 °C, 5% CO_2. Again, an 8 µL viral droplet was placed in a 15 mL sterile polypropylene tube as a negative control. After incubation, the samples were carefully placed in 15 mL tubes containing 2 mL of serum-free DMEM, using sterile equipment. Similarly, in the case of the negative controls, 2 mL of serum-free DMEM was added to the tube containing the viral droplet. All tubes were then vortexed for one minute to release the virions into the medium, which was then used to infect A549 cells.

2.5 Cell infection

Prior to the infection experiments, the cells were seeded in 24-well plates at 80,000 cells/well in DMEM/FCS/PenStrep and incubated overnight at 37 °C, 5% CO_2. The following day, the medium was carefully aspirated and the cells were washed once with serum-free DMEM. Then, 300 µL of the viral supernatants were added to the cells and the plate was incubated for one hour at 37 °C, 5% CO_2. The plate was gently shaken every 15 minutes to ensure the virions were brought uniformly into contact with the cells. After incubation, the viral solutions were carefully removed, the cells were washed once with

serum-free DMEM, and DMEM/FCS/PenStrep was added. The cells were then incubated for 22–24 hours at 37 °C, 5% CO_2. After that, the medium was removed and the cells were carefully washed once with phosphate-buffered saline (PBS, Sigma-Aldrich, St. Louis, MO, USA).

2.6 Infectivity assay

To assess the amount of virus still infectious after material treatment, the Dual-Luciferase Reporter Assay System (DLR) (Promega, Madison, WI, USA) was used. When virions infect human cells, they shed their capsid and express viral genes using the cell's machinery [40]. The principle behind the assay is that as more cells are infected, more of the luminescent reporter protein luciferase is expressed from the gene inserted into the viral genome. Thus, luminescence can be positively correlated with the amount of infectious virus. The cell samples were then analysed according to the DLR protocol. Luminescence was measured using an Infinite M200 luminometer (Tecan, Männedorf, Switzerland).

2.7 Statistical analysis

Quantitative data are reported as mean ± standard deviation (SD). A one-way Welch analysis of variance (ANOVA) with Games–Howell post-hoc tests was used to identify significant differences between test and control groups, in IBM SPSS Statistics (IBM Corp., Armonk, NY, USA). A significance level of $p = 0.05$ was set for all tests. Effect sizes were calculated as eta-squared (η^2) to supplement the inferential statistics.

3 Results and discussion

3.1 Powders

XRD measurements of the as-received silicon nitride powder indicated that it was comprised mostly of particles of the α-phase (Figure 1(c)). This was also morphologically evident through SEM imaging (Figure 1(a)), as most particles were equiaxed, with only a few exhibiting the characteristic rod-like morphology of the β-phase. The powder consisted of sub-micron particles that formed a few soft agglomerates, hypothesised to be easily dispersed when in suspension. The particle size of the copper positive control was significantly larger, with spherical particles that also formed agglomerates (Figure 1(b)).

The apparent total surface area of the silicon nitride particles in suspension was higher than that of the copper control powder due to its lower mass density (3.17 g/cm^3 versus 8.96 g/cm^3, respectively), its smaller particle size, and its edged morphology. Consequently, more contact between the powder and the virus likely occurred for the silicon nitride samples at the same weight-per-volume concentration. This may be important in interpreting the results.

To measure the effect of silicon nitride on adenovirus infectivity, the powder was mixed with a solution containing HAdV-5. The infectivity of the viral solutions after 1-, 10- and 60-minute treatment was compared with that of the untreated viral solution and copper controls (Figure 2). The results of the luciferase assay indicated that silicon nitride had a clear inactivating effect on the HAdV-5 virions. After 1 minute of treatment with the Si_3N_4 powder, overall infectivity was reduced by more than 98%. This showed that the chemistry of silicon nitride significantly reduced viral activity, as hypothesised. Interestingly, these inactivation rates were as efficient as those observed after silicon nitride treatment of the much more fragile ssRNA viruses, such as SARS-CoV-2 [25, 41].

A comparison of the capacity of silicon nitride and copper to inactivate HAdV-5 indicated that both substances were effective. However, silicon nitride showed a consistent, strong effect at all times tested, whereas the effect of copper increased with contact time (Figure 2).

This observation may be due to the different mass densities and particle sizes of Si_3N_4 and copper, as well as the time-dependent release of copper ions from the copper powders. As shown in Figure 3, the efficacy of copper to inhibit infection correlated with its release of ions, whereas silicon nitride showed a consistently high efficiency over time, indicating that the inactivating mechanism of the material achieved sufficient viral inactivation in as little as one minute of contact. The lower density and smaller particle size of silicon nitride mean that, for the same mass, more powder particles of the material are brought into contact with virions. Taking into consideration the 'catch and kill' mechanism of the antiviral action of silicon nitride discussed later, this could result in more rapid viral inactivation.

The antiviral behaviour of copper stems mainly from the release of copper ions and secondarily from the action of reactive oxygen species [42]. The underlying ionic mechanisms, involving both Cu(I) and Cu(II) species, have been characterised in studies of copper-bearing antimicrobial materials [43], and

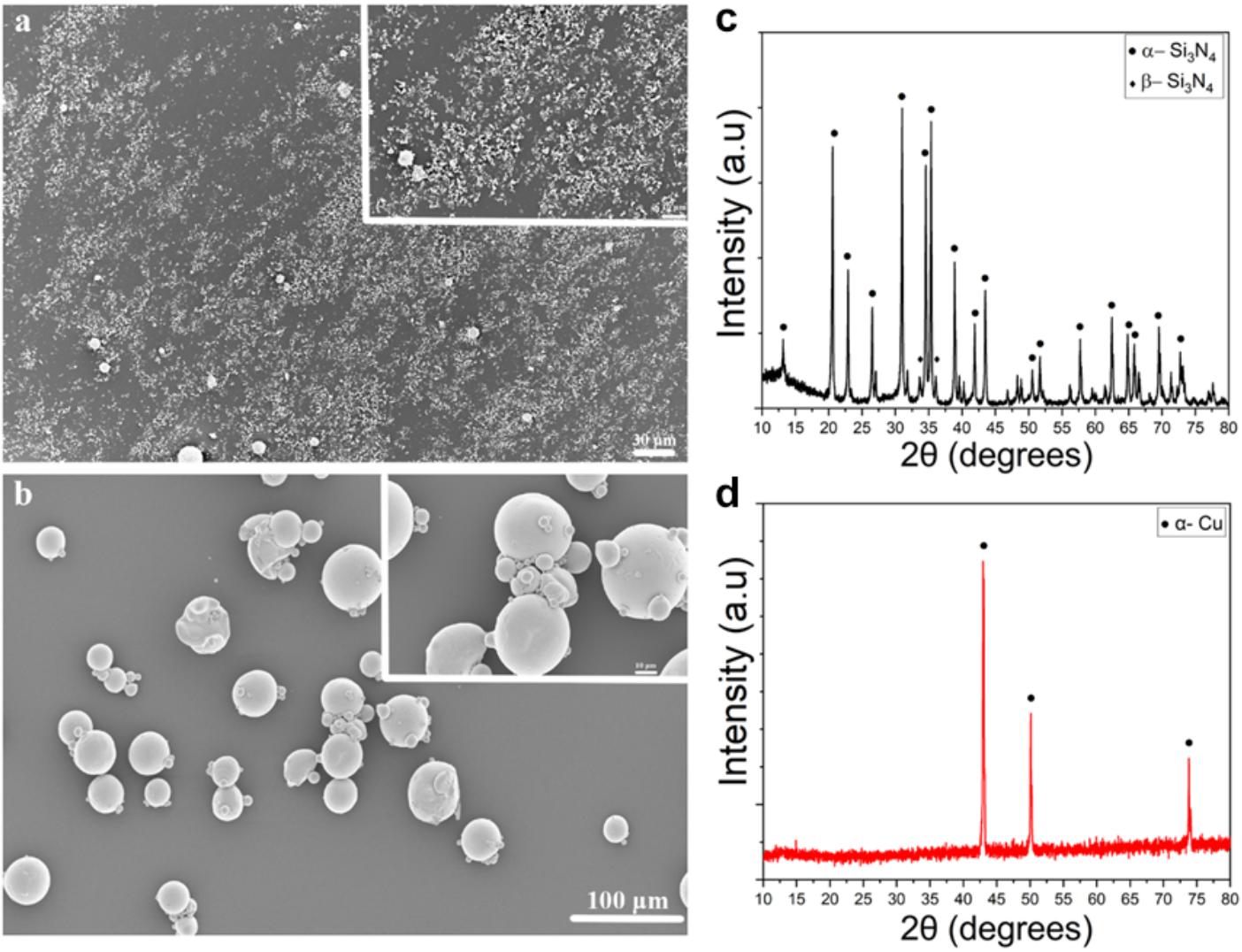

Figure 1. SEM images showing the morphology of the (a) silicon nitride and (b) copper powders. The larger background images were taken at 500× magnification while the inset images were taken at 2000× magnification. XRD confirmed that (c) the silicon nitride powders were mainly α-phase, as evidenced by the low intensity of peaks belonging to the β-phase, and (d) the copper powder was α-Cu.

copper ions of both species have been shown to damage the viral genome and inactivate viruses. ICP-OES measurements showed that the release of the virucidal copper ions is clearly time-dependent, which explains the reduction in infective virions as contact time increased.

Another interesting observation was made regarding the crystallinity of the material. Our study used α-phase Si_3N_4, whereas the studies on RNA viruses have used mostly β-phase Si_3N_4 in the tested suspensions. The two phases differ significantly in their morphologies, with the α-phase having relatively equiaxed particles while the β-phase exhibits rod-like elongated particles. These morphologies have different surface areas, and their effect on antipathogenic properties is unclear. However, the current findings indicate that the antiviral effect of silicon nitride is largely independent of the material's phase composition; the mechanism is mainly due to its chemistry. Nevertheless, a study directly comparing α- and β-phase powders in the same experiment is needed to confirm this indication.

3.2 Surfaces

XRD measurements of the sintered silicon nitride surfaces demonstrated that the surface was mainly comprised of β-phase grains (Figure 4). The sintering parameters used, as detailed by Fu et al. [38], were optimised to achieve an α- to β-phase transformation that is favourable for the material's mechanical properties [38, 44]. The relative density of the samples

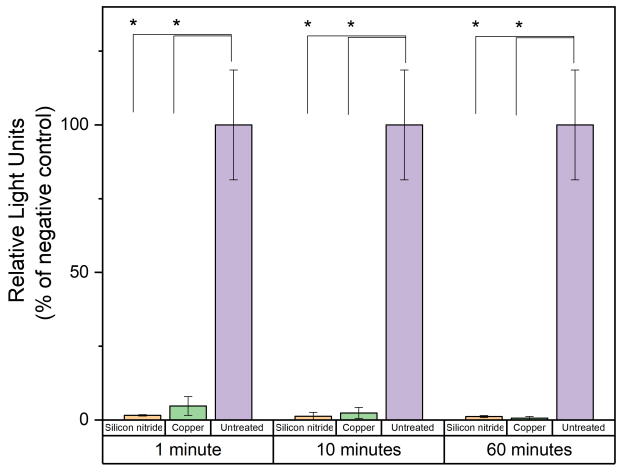

Figure 2. The results of the luciferase assay for the test powders and controls after one, 10 and 60 minutes of contact indicated a statistically significant loss of infectivity in virus solutions treated with Si_3N_4 ($p < 0.006$ in all cases) and Cu ($p < 0.005$ in all cases) when compared with the untreated control.

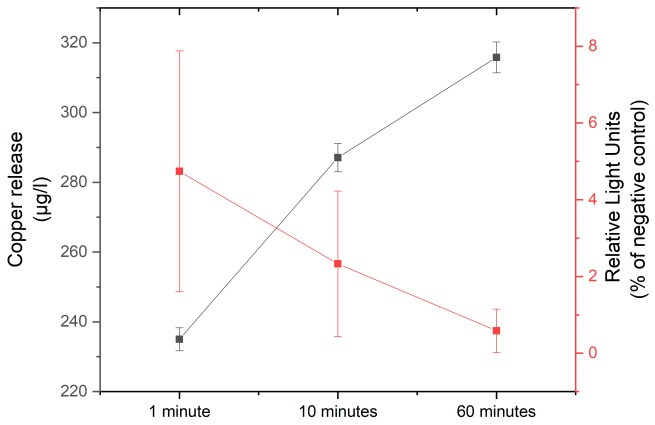

Figure 3. The results of the luciferase assay showed a clear time dependency of the inactivating capability of the copper powders. The release of copper ions by the powders showed an inverse relationship to viral infectivity (i.e., increasing ion release accompanied increasing inactivation).

was 92.2% [38]. Pathogen attachment to surfaces, including that of bacteria, has been shown [45, 46] to be positively correlated with surface roughness, a principle that has been extended to viral adhesion on material surfaces. The optical profilometry measurements demonstrated that the silicon nitride samples had an average surface roughness (S_a) of 89.7 ± 55 nm, while that of copper was 19.3 ± 7 nm. The relatively large standard deviation observed for silicon nitride is attributed to the heterogeneous microstructure resulting from the spark plasma sintering process, which produces local variations in grain size and porosity across the surface. Thus, the higher nanoscale roughness of the silicon nitride surfaces could lead to higher attachment of virions to the surface.

The inactivating effect of silicon nitride on DNA virions in bulk form has not yet been investigated. While it is reasonable to hypothesise that the material would act similarly in bulk form, the rate of inactivation is still important to explore. The material in powder form has a higher surface area, which provides a greater rate of interaction between the material and the virions.

The starting hypothesis was that silicon nitride surfaces would still have an inactivating effect, although lower than that observed for powders. The results of the luciferase inactivation assay confirmed that a statistically significant reduction of viral infectivity occurred after a 10-minute contact with silicon nitride (73% inactivation, $p = 0.008$) (Figure 5). This value was only marginally increased after a prolonged contact of 60 minutes (75% inactivation, $p = 0.045$) (Figure 5). Both values suggest that bulk silicon nitride inactivates the virus, although less efficiently than silicon nitride powders (Figure 2). In the case of copper, almost no viral activity could be detected. This could be due to a combination of the virucidal effectiveness of copper and its inherent cell toxicity, as a cytopathic effect was noticed, making fewer cells available for infection. These inactivation rates, while lower than those of the powdered material, are still significant for some applications. The material can be used on common touch surfaces to reduce microbial load.

Studies by Pezzotti et al. [25, 41, 47] have described a possible mechanism for the antiviral action of silicon nitride on different ssRNA viruses. The authors proposed a 'catch and kill' mechanism in which the silicon nitride materials initially bind to virions through electrical charge attraction and the formation of Si–NH_3^+ groups that resemble lysine terminals, a viral receptor on cells. After binding, the eluted ammonia ions penetrate the virion, damaging the genomic RNA, which is susceptible to degradation by ammonia [48]. The damage to the RNA was proposed to occur through alkaline transesterification. In our study, we observed that the silicon nitride treatment also effectively inactivated the human adenovirus.

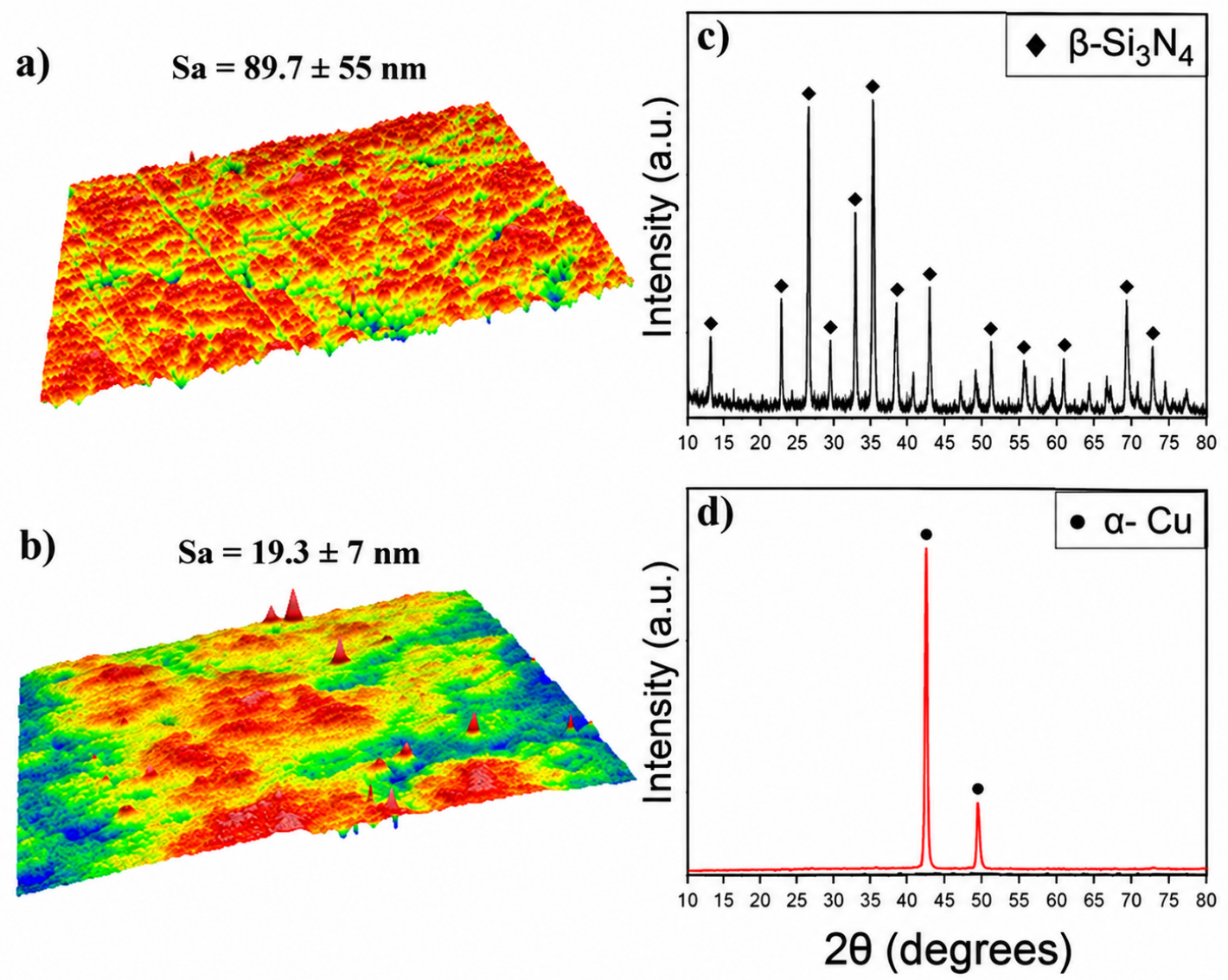

Figure 4. The surface and crystallographic characterization of silicon nitride (a, c) and copper (b, d) surfaces. Silicon nitride surfaces were rougher than copper surfaces.

The adenovirus, in contrast to the tested ssRNA viruses, is a non-enveloped DNA virus. Therefore, since DNA lacks the 2′-OH hydroxyl group found on RNA, it cannot undergo the alkaline transesterification possible for RNA viruses. In the case of the adenovirus, the inactivation is more likely an effect of the interaction of eluted ammonia ions with the viral capsid. The subsequent degradation of the viral proteins would result in the release of the naked viral DNA, which is essentially non-infectious.

One limitation of this study concerns the experimental procedures during the recording of the material–virus contact time. On close examination of the protocol, one notices that after the elapsed contact time there was a processing time, mainly centrifuging and vortexing, to separate the virus from the test materials. It seems possible that interaction between the materials and the virions continued throughout the processing time, making the contact times reported in the results underestimated. Hence, one should be careful in interpreting the results if time dependence is important for the envisaged applications. Protocols with stricter control of the contact time should be designed in future experiments.

This study supports the currently published evidence for the use of silicon nitride as a biocidal material. The material has been shown to be effective against fungi [49], bacteria [50] and ssRNA viruses [25]. With this study confirming the effectiveness of the material against DNA viruses, it is clear that silicon nitride can be crucial in reducing the pathogenic load in a variety of applications. Using the material in bulk form or

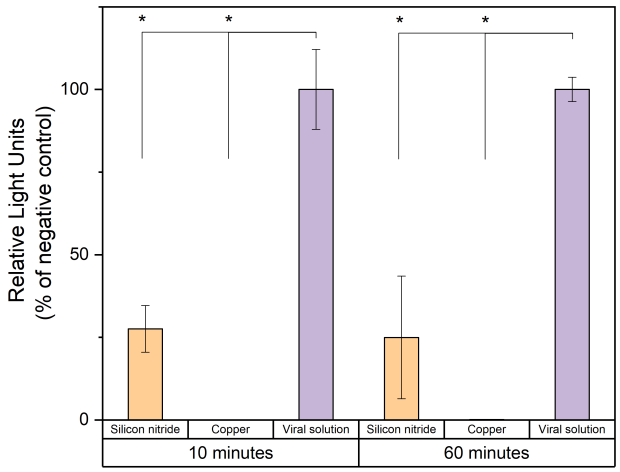

Figure 5. The results of the luciferase assay for surfaces and controls after 10 and 60 minutes showed that the silicon nitride treatment had an inhibiting effect on viral infectivity after as little as 10 minutes of contact.

as a coating on common touch surfaces can lead to containment of viral and bacterial spread. Copper has been found to be effective in such applications [12, 13]; thus, the biocompatible silicon nitride [15, 16] could provide an alternative. In powder form, the material can be integrated into disinfecting solutions, polymeric matrices and fabrics, lending them its antipathogenic properties. In this study, both powder and bulk ceramic samples were tested and showed different effectiveness. The powder demonstrated better inactivation, mainly because of its particle shape and high surface area, which more readily react with water and further interact with viruses. Another reason may be the different phases of silicon nitride, the powder being in the α-phase and the bulk ceramic in the β-phase. There is no clear evidence as to which phase has the faster reaction rate with water to generate reactive nitrogen species. However, considering crystal structure and thermal stability, α-silicon nitride is less stable than β-silicon nitride. Heath et al. [51] recently reported that the antiviral effect of α-silicon nitride powder was greater than that of β-silicon nitride powder, albeit for slightly different powder sizes: 0.68 µm (α-phase) and 0.89 µm (β-phase). Notably, the α-phase powder used in the present study had a D_{50} of 0.856 µm, which falls between these two sizes, suggesting that particle size alone is unlikely to account for the observed phase-dependent differences in antiviral efficacy. With the effectiveness and mode of action known, the next step towards application of the material would be to tailor its properties to specific applications. Enhancing the effect of the material without compromising its mechanical properties may be possible, e.g., through (i) grain-size control to increase boundary density and interaction with water; (ii) introduction of antibacterial sintering additives; and (iii) surface roughness and topography modifications to increase surface area. In this way, the applicability of the material will be enhanced, limiting the spread of pathogens and the diseases they cause.

4 Conclusion

In this study, we examined the effect of silicon nitride, in both bulk and powder forms, on the infectivity of the adenovirus, a stable DNA virus. Both forms of the material resulted in a significant reduction of its infectivity. This suggests that the material is effective against one of the sturdiest human DNA viruses characterised, even in bulk form, something that has not previously been shown. This study further suggests that silicon nitride materials will be effective in the fight against a wide range of viral pathogens.

Data Availability Statement

Data will be made available on request.

Funding

This work was supported by the Vinnova under Grant 2020-03099; by the European Union's Horizon 2020 Research and Innovation Programme under the Marie Skłodowska-Curie Grant Agreement No. 812765; and by the Swedish Cancer Foundation under Grant 180599. The authors would also like to thank "Wefightcovid" (SPR) for their financial donation in support of this research.

Conflicts of Interest

Wei Xia served as an Editorial Board Member of the *Journal of Advanced Materials Research* at the time of manuscript submission. To ensure the integrity of the peer-review process, Wei Xia was not involved in the editorial handling, peer review, or decision-making process for this manuscript, which was handled independently by another editor. The remaining authors declare no conflicts of interest.

AI Use Statement

The authors declare that no generative AI was used in the preparation of this manuscript.

Ethical Approval and Consent to Participate

Not applicable.

References

[1] Piret, J., & Boivin, G. (2021). Pandemics throughout history. *Frontiers in microbiology, 11*, 631736. [CrossRef]

[2] Petersen, E., Koopmans, M., Go, U., Hamer, D. H., Petrosillo, N., Castelli, F., ... & Simonsen, L. (2020). Comparing SARS-CoV-2 with SARS-CoV and influenza pandemics. *The Lancet infectious diseases, 20*(9), e238-e244. [CrossRef]

[3] Imani, S. M., Ladouceur, L., Marshall, T., Maclachlan, R., Soleymani, L., & Didar, T. F. (2020). Antimicrobial nanomaterials and coatings: current mechanisms and future perspectives to control the spread of viruses including SARS-CoV-2. *ACS nano, 14*(10), 12341-12369. [CrossRef]

[4] Wu, F., Zhao, S., Yu, B., Chen, Y. M., Wang, W., Song, Z. G., ... & Zhang, Y. Z. (2020). A new coronavirus associated with human respiratory disease in China. *Nature, 579*(7798), 265-269. [CrossRef]

[5] Rothan, H. A., & Byrareddy, S. N. (2020). The epidemiology and pathogenesis of coronavirus disease (COVID-19) outbreak. *Journal of autoimmunity, 109*, 102433. [CrossRef]

[6] Pradhan, D., Biswasroy, P., Naik, P. K., Ghosh, G., & Rath, G. (2020). A review of current interventions for COVID-19 prevention. *Archives of medical research, 51*(5), 363-374. [CrossRef]

[7] Liao, M., Liu, H., Wang, X., Hu, X., Huang, Y., Liu, X., ... & Lu, J. R. (2021). A technical review of face mask wearing in preventing respiratory COVID-19 transmission. *Current Opinion in Colloid & Interface Science, 52*, 101417. [CrossRef]

[8] Tang, Z., Kong, N., Zhang, X., Liu, Y., Hu, P., Mou, S., ... & Tao, W. (2020). A materials-science perspective on tackling COVID-19. *Nature Reviews Materials, 5*(11), 847-860. [CrossRef]

[9] Kramer, A., Schwebke, I., & Kampf, G. (2006). How long do nosocomial pathogens persist on inanimate surfaces? A systematic review. *BMC infectious diseases, 6*(1), 130. [CrossRef]

[10] Van Doremalen, N., Bushmaker, T., & Munster, V. J. (2013). Stability of Middle East respiratory syndrome coronavirus (MERS-CoV) under different environmental conditions. *Eurosurveillance, 18*(38), 20590. [CrossRef]

[11] Chatterjee, P., Williams, M. D., Coppin, J. D., Allton, Y., Choi, H., Martel, J. A. D., ... & Jinadatha, C. (2020, August). Effectiveness of copper-impregnated solid surfaces on lowering microbial bio-burden levels in an acute care hospital. In *Open forum infectious diseases* (Vol. 7, No. 8, p. ofaa238). US: Oxford University Press. [CrossRef]

[12] Colin, M., Klingelschmitt, F., Charpentier, E., Josse, J., Kanagaratnam, L., De Champs, C., & Gangloff, S. C. (2018). Copper alloy touch surfaces in healthcare facilities: An effective solution to prevent bacterial spreading. *Materials, 11*(12), 2479. [CrossRef]

[13] Ibrahim, Z., Petrusan, A. J., Hooke, P., & Hinsa-Leasure, S. M. (2018). Reduction of bacterial burden by copper alloys on high-touch athletic center surfaces. *American journal of infection control, 46*(2), 197-201. [CrossRef]

[14] Riley, F. L. (2000). Silicon nitride and related materials. *Journal of the American Ceramic Society, 83*(2), 245-265. [CrossRef]

[15] Kue, R., Sohrabi, A., Nagle, D., Frondoza, C., & Hungerford, D. (1999). Enhanced proliferation and osteocalcin production by human osteoblast-like MG63 cells on silicon nitride ceramic discs. *Biomaterials, 20*(13), 1195-1201. [CrossRef]

[16] Neumann, A., Reske, T., Held, M., Jahnke, K., Ragoss, C., & Maier, H. R. (2004). Comparative investigation of the biocompatibility of various silicon nitride ceramic qualities in vitro. *Journal of Materials Science: Materials in Medicine, 15*(10), 1135-1140. [CrossRef]

[17] Bal, B. S., & Rahaman, M. N. (2012). Orthopedic applications of silicon nitride ceramics. *Acta biomaterialia, 8*(8), 2889-2898. [CrossRef]

[18] Bocanegra-Bernal, M. H., & Matovic, B. (2010). Mechanical properties of silicon nitride-based ceramics and its use in structural applications at high temperatures. *Materials Science and Engineering: A, 527*(6), 1314-1338. [CrossRef]

[19] Kersten, R. F. M. R., Öner, F. C., Arts, M. P., Mitroiu, M., Roes, K. C. B., De Gast, A., & Van Gaalen, S. M. (2022). The SNAP trial: 2-year results of a double-blind multicenter randomized controlled trial of a silicon nitride versus a PEEK cage in patients after lumbar fusion surgery. *Global Spine Journal, 12*(8), 1687-1695. [CrossRef]

[20] Arts, M. P., Wolfs, J. F., & Corbin, T. P. (2017). Porous silicon nitride spacers versus PEEK cages for anterior cervical discectomy and fusion: clinical and radiological results of a single-blinded randomized controlled trial. *European Spine Journal, 26*(9), 2372-2379. [CrossRef]

[21] Du, X., Lee, S. S., Blugan, G., & Ferguson, S. J. (2022). Silicon nitride as a biomedical material: an overview. *International Journal of Molecular Sciences, 23*(12), 6551. [CrossRef]

[22] Wu, J., Liu, Y., Zhang, H., Wu, Y., Chu, Z., Wu, Q., ... & Tang, C. (2021). Silicon nitride as a potential candidate for dental implants: Osteogenic activities and antibacterial properties. *Journal of Materials Research, 36*(9), 1866-1882. [CrossRef]

[23] Webster, T. J., Patel, A. A., Rahaman, M. N., & Bal, B. S. (2012). Anti-infective and osteointegration properties of silicon nitride, poly (ether ether ketone), and

titanium implants. *Acta biomaterialia, 8*(12), 4447-4454. [CrossRef]

[24] Pezzotti, G., Bock, R. M., McEntire, B. J., Jones, E., Boffelli, M., Zhu, W., ... & Bal, B. S. (2016). Silicon nitride bioceramics induce chemically driven lysis in Porphyromonas gingivalis. *Langmuir, 32*(12), 3024-3035. [CrossRef]

[25] Pezzotti, G., Boschetto, F., Ohgitani, E., Fujita, Y., Zhu, W., Marin, E., ... & Mazda, O. (2021). Silicon nitride: a potent solid-state bioceramic inactivator of ssRNA viruses. *Scientific Reports, 11*(1), 2977. [CrossRef]

[26] Simpson, S., McMinn, C., Van Mondfrans, S. M., Hendry, J., Ronayne, S., Dewhurst, S., ... & McEntire, B. J. (2023). A novel Antipathogenic agent for nonwoven fabric. *Biomedical Materials & Devices, 1*(1), 469-482. [CrossRef]

[27] Sanjuán, R., & Domingo-Calap, P. (2016). Mechanisms of viral mutation. *Cellular and molecular life sciences, 73*(23), 4433-4448. [CrossRef]

[28] Enriquez, C. E., Hurst, C. J., & Gerba, C. P. (1995). Survival of the enteric adenoviruses 40 and 41 in tap, sea, and waste water. *Water Research, 29*(11), 2548-2553. [CrossRef]

[29] Khanal, S., Ghimire, P., & Dhamoon, A. S. (2018). The repertoire of adenovirus in human disease: the innocuous to the deadly. *Biomedicines, 6*(1), 30. [CrossRef]

[30] Ganime, A. C., Carvalho-Costa, F. A., Santos, M., Costa Filho, R., Leite, J. P. G., & Miagostovich, M. P. (2014). Viability of human adenovirus from hospital fomites. *Journal of medical virology, 86*(12), 2065-2069. [CrossRef]

[31] Dodge, M. J., MacNeil, K. M., Tessier, T. M., Weinberg, J. B., & Mymryk, J. S. (2021). Emerging antiviral therapeutics for human adenovirus infection: Recent developments and novel strategies. *Antiviral research, 188*, 105034. [CrossRef]

[32] Louie, J. K., Kajon, A. E., Holodniy, M., Guardia-LaBar, L., Lee, B., Petru, A. M., ... & Schnurr, D. P. (2008). Severe pneumonia due to adenovirus serotype 14: a new respiratory threat?. *Clinical infectious diseases, 46*(3), 421-425. [CrossRef]

[33] Dai, M., Wu, Y., Tan, H., Deng, J., Hou, M., Peng, W., ... & Lu, J. (2020). Cross-infection of adenovirus among medical staff: A warning from the intensive care unit in a tertiary care teaching hospital in China. *International Journal of Infectious Diseases, 98*, 390-397. [CrossRef]

[34] Thompson, S. S., Jackson, J. L., Suva-Castillo, M., Yanko, W. A., El Jack, Z., Kuo, J., ... & Schnurr, D. P. (2003). Detection of infectious human adenoviruses in tertiary-treated and ultraviolet-disinfected wastewater. *Water Environment Research, 75*(2), 163-170. [CrossRef]

[35] Thurston-Enriquez, J. A., Haas, C. N., Jacangelo, J., Riley, K., & Gerba, C. P. (2003). Inactivation of feline calicivirus and adenovirus type 40 by UV radiation. *Applied and Environmental Microbiology, 69*(1), 577-582. [CrossRef]

[36] Grass, G., Rensing, C., & Solioz, M. (2011). Metallic copper as an antimicrobial surface. *Applied and environmental microbiology, 77*(5), 1541-1547. [CrossRef]

[37] Borkow, G., & Gabbay, J. (2005). Copper as a biocidal tool. *Current medicinal chemistry, 12*(18), 2163-2175. [CrossRef]

[38] Fu, L., Xiong, Y., Carlsson, G., Palmer, M., Örn, S., Zhu, W., ... & Xia, W. (2018). Biodegradable Si3N4 bioceramic sintered with Sr, Mg and Si for spinal fusion: Surface characterization and biological evaluation. *Applied Materials Today, 12*, 260-275. [CrossRef]

[39] Mittal, S. K., McDermott, M. R., Johnson, D. C., Prevec, L., & Graham, F. L. (1993). Monitoring foreign gene expression by a human adenovirus-based vector using the firefly luciferase gene as a reporter. *Virus research, 28*(1), 67-90. [CrossRef]

[40] Ryu, W. S. (2016). Virus life cycle. In *Molecular virology of human pathogenic viruses* (pp. 31-50). Academic Press. [CrossRef]

[41] Pezzotti, G., Ohgitani, E., Shin-Ya, M., Adachi, T., Marin, E., Boschetto, F., ... & Mazda, O. (2020). Instantaneous "catch-and-kill" inactivation of SARS-CoV-2 by nitride ceramics. *Clinical and translational medicine, 10*(6), e212. [CrossRef]

[42] Sunada, K., Minoshima, M., & Hashimoto, K. (2012). Highly efficient antiviral and antibacterial activities of solid-state cuprous compounds. *Journal of hazardous materials, 235*, 265-270. [CrossRef]

[43] Nan, L., Liu, Y., Lü, M., & Yang, K. (2008). Study on antibacterial mechanism of copper-bearing austenitic antibacterial stainless steel by atomic force microscopy. *Journal of Materials Science: Materials in Medicine, 19*(9), 3057-3062. [CrossRef]

[44] Han, W., Li, Y., Chen, G., & Yang, Q. (2017). Effect of sintering additive composition on microstructure and mechanical properties of silicon nitride. *Materials Science and Engineering: A, 700*, 19-24. [CrossRef]

[45] Goulter-Thorsen, R. M., Taran, E., Gentle, I. R., Gobius, K. S., & Dykes, G. A. (2011). Surface roughness of stainless steel influences attachment and detachment of Escherichia coli O157. *Journal of food protection, 74*(8), 1359-1368. [CrossRef]

[46] Cheng, Y., Feng, G., & Moraru, C. I. (2019). Micro-and nanotopography sensitive bacterial attachment mechanisms: a review. *Frontiers in microbiology, 10*, 191. [CrossRef]

[47] Pezzotti, G., Boschetto, F., Ohgitani, E., Fujita, Y., Shin-Ya, M., Adachi, T., ... & Mazda, O. (2021). Mechanisms of instantaneous inactivation of SARS-CoV-2 by silicon nitride bioceramic. *Materials Today Bio, 12*, 100144. [CrossRef]

[48] Decrey, L., Kazama, S., Udert, K. M., & Kohn, T. (2015). Ammonia as an in situ sanitizer: inactivation kinetics and mechanisms of the ssRNA virus MS2 by NH3. *Environmental Science & Technology, 49*(2), 1060-1067. [CrossRef]

[49] Pezzotti, G., Asai, T., Adachi, T., Ohgitani, E., Yamamoto, T., Kanamura, N., ... & Nishimura, I. (2021). Antifungal activity of polymethyl methacrylate/Si3N4 composites against Candida albicans. *Acta Biomaterialia, 126*, 259-276. [CrossRef]

[50] Bock, R. M., Jones, E. N., Ray, D. A., Sonny Bal, B., Pezzotti, G., & McEntire, B. J. (2017). Bacteriostatic behavior of surface modulated silicon nitride in comparison to polyetheretherketone and titanium. *Journal of Biomedical Materials Research Part A, 105*(5), 1521-1534. [CrossRef]

[51] Heath, B. N., Woodson, C. M., McMinn, C., Bock, R. M., & Kehn-Hall, K. (2025). Antiviral efficacy of silicon nitride against SARS-CoV-2 and MERS-CoV: implications for PPE innovation. *Frontiers in Microbiology, 16*, 1637848. [CrossRef]